Quantitative Real-Time PCR Method for Detection of B-Lymphocyte Monoclonality by Comparison of κ and λ Immunoglobulin Light Chain Expression

ANDERS STÅHLBERG,[1] PIERRE ÅMAN,[2] BÖRJE RIDELL,[2] PETTER MOSTAD,[3] and
MIKAEL KUBISTA[1,4*]

Background: An abnormal IgLκ:IgLλ ratio has long been used as a clinical criterion for non-Hodgkin B-cell lymphomas. As a first step toward a quantitative real-time PCR-based multimarker diagnostic analysis of lymphomas, we have developed a method for determination of IgLκ:IgLλ ratio in clinical samples.

Methods: Light-up probe-based real-time PCR was used to quantify IgLκ and IgLλ cDNA from 32 clinical samples. The samples were also investigated by routine immunohistochemical analysis and flow cytometry.

Results: Of 32 suspected non-Hodgkin lymphoma samples analyzed, 28 were correctly assigned from real-time PCR measurements assuming invariant PCR efficiencies in the biological samples. Four samples were false negatives. One was a T-cell lymphoma, one was a diffuse large B-cell lymphoma, and one was reanalyzed and found lymphoma-positive by in situ calibration, which takes into account sample-specific PCR inhibition. Twelve of the samples were fine-needle aspirates, and these were all correctly assigned.

Conclusions: This work is a first step toward analyzing clinical samples by quantitative light-up probe-based real-time PCR. Quantitative real-time PCR appears suitable for high-throughput testing of cancers by measuring expression of tumor markers in fine-needle aspirates.
© 2003 American Association for Clinical Chemistry

The rapid expansion in knowledge of the human genome and the development of techniques for analysis of nucleic acids have opened new possibilities for diagnostics. In our first attempt to use quantitative real-time PCR (Q-PCR)[5] for detection of malignant tumors, we have focused on the analysis of non-Hodgkin lymphomas (NHLs).

The vast majority of NHLs develop from a B-lymphocyte lineage. B-lymphocytes produce immunoglobulins with a heavy chain and either a κ (IgLκ) or a λ (IgLλ) light chain. Which light chain will be produced is determined early in the development of each B-lymphocyte. In healthy humans, ~60% of B-cells produce κ chains and the rest produce λ chains. Normal lymphoid tissues therefore contain a mixture of B-cells with an IgLκ:IgLλ ratio of ~60:40 *(1, 2)*.

Lymphomas, like all malignant tumors, are clonal and arise from one transformed cell. Lymphoma tissues are dominated by the tumor cells; consequently, the IgLκ:IgLλ ratio is changed. With κ-producing tumors, the IgLκ:IgLλ ratio is higher, whereas with λ-producing tumors, the ratio is lower. Assuming that the translation efficiency and stability of the IgLκ and IgLλ mRNAs are similar, clonality may be detected by measuring the IgLκ:IgLλ expression ratio.

Real-time PCR can detect and quantify target nucleic acids in biological samples with light-up probes *(3–5)*. We have used this approach to assess the expression of IgLκ and IgLλ in B-cell lymphoid tumors. Although it cannot yet replace traditional immunohistochemistry (IHC) and flow cytometry in diagnosis, this assay, which takes into

Departments of [1] Molecular Biotechnology and [3] Mathematics, Chalmers University of Technology, 405 30 Gothenburg, Sweden.
[2] Department of Pathology, Lundberg Laboratory for Cancer Research, Gothenburg University, 413 45 Gothenburg, Sweden.
[4] TATAA Biocenter, Chalmers University of Technology, 405 30 Gothenburg, Sweden.
*Address correspondence to this author at: TATAA Biocenter, Medicinarg. 9C, Chalmers University of Technology, 405 30 Gothenburg, Sweden. Fax 46-31-7733948; e-mail mikael.kubista@tataa.com.

[5] Nonstandard abbreviations: Q-PCR, quantitative PCR; NHL, non-Hodgkin lymphoma; IgLκ and IgLλ, immunoglobulin, κ and λ light chains, respectively; IHC, immunohistochemistry; CT, threshold cycle number; and dNTP, deoxynucleotide triphosphate.

account reaction efficiency, demonstrates the potential of quantitative reverse transcription-PCR in cancer diagnostics.

Material and Methods

SAMPLE COLLECTION

Surgical lymph node biopsies from previously untreated patients were transported from the operation theatre in ice-water-chilled boxes and handled in the laboratory within 30 min. Material for the study was rapidly frozen in dry ice/isopentane and stored at −70 °C. Samples BR101–BR112 were fine-needle aspirates suspended in RNAlater (Ambion) directly at the time of sample collection. The cell suspension was stored in RNAlater at 4 °C for 1 or 2 days before the cells were collected by centrifugation and stored frozen at −80 °C. Parts of the tissues were fixed in formalin and used for routine diagnostic analysis. Diagnosis was reached by a combination of microscopic histologic evaluation; immunostaining of several markers, including the κ and λ chains (IHC); and in some cases, flow cytometry. The samples were classified as lymphadenitis or malignant lymphoma according to the Revised European-American Lymphoma classification system (6).

RNA EXTRACTION AND cDNA SYNTHESIS

RNA was extracted by use of the Fast Prep System (FastRNA Green; Qbiogene). We mixed 10 μg of total RNA with 2 μg of poly(dT) oligomers (Pharmacia) and incubated the mixture at 65 °C for 5 min. First-strand cDNA synthesis was then performed by adding 0.05 mol/L Tris-HCl (pH 8.3), 0.075 mol/L KCl, 3 mmol/L MgCl$_2$, 0.01 mol/L dithiothreitol, 10 U/mL Moloney murine leukemia virus reverse transcriptase (Life Technologies), 0.05 units/mL RNA guard (Life Technologies), and 10 mmol/L of each deoxyribonucleotide (Life Technologies) to a final volume of 20 μL and incubating the samples at 37 °C for 1 h. The reaction was terminated by incubation at 65 °C for 5 min, and samples were stored at −80 °C.

LIGHT-UP PROBES

Two homopyrimidine light-up probes, H-CCTTTTTCCC-NH$_2$ (IgLκLUP) and CCTCCTCTCT-NH2 (IgLλLUP), directed against PCR amplification products of the constant regions in the human IgLκ and IgLλ light chains, respectively, were designed. Both probes are homopyrimidine sequences, which are known to exhibit very large signal enhancement on target binding (7). Both probes had the thiazole orange derivative, N-carboxypentyl-4-[(3′-methyl-1′,3′-benzothiazol-2′-yl)methylenyl]quinolinium iodide, as label attached to the peptide nucleic acid. They were synthesized by solid-phase synthesis and purified twice by reversed-phase HPLC as described previously (8). Probe concentrations were determined spectroscopically assuming molar absorptivities at 260 nm of 83 100 M^{-1} cm^{-1} for IgLκLUP and 81 100 M^{-1} cm^{-1} for IgLλLUP (8). The probes were designed to have melting temperatures of 65–70 °C, which is between the annealing (55 °C) and elongation (74 °C) temperatures of the PCRs.

PCR PRODUCTS

PCR products were purified with a QIAquick^{TM} PCR purification reagent set (Qiagen), and their concentrations were determined spectroscopically, assuming a molar absorptivity at 260 nm of 13 200 M^{-1} cm^{-1} per base pair (9). Primer (Medprobe Inc.) concentrations were estimated assuming: $\epsilon_{260}/10^3 = 12.0 \cdot n_G + 7.1 \cdot n_C + 15.2 \cdot n_A + 8.4 \cdot n_T$ M^{-1} cm^{-1}, where n_X is the total number of base X (9).

REAL-TIME PCR

PCR systems were designed for a 231-bp fragment of human IgLκ (GenBank accession no. AK024974) and a 223-bp fragment of human IgLλ (GenBank accession no. X51755), which comprise the IgLκLUP and IgLλLUP target sequences, respectively.

Reaction conditions were optimized as described elsewhere (10). IgLκ and IgLλ PCRs both contained 75 mM Tris (pH 8.8), 20 mM (NH$_4$)$_2$SO$_4$, 1 mL/L Tween 20, 1 U of JumpStart^{TM} Taq DNA polymerase (with antibody; Sigma-Aldrich), and 200 ng/μL bovine serum albumin (Fermentas). Specific components for the IgLκ PCR were 5 mM MgCl$_2$, 0.2 mM deoxyribonucleotides (Sigma-Aldrich), 800 nM each of the primers (MedProbe Inc.), and 800 nM IgLκLUP; for the IgLλ PCR, specific components were 3.5 mM MgCl$_2$, 0.4 mM deoxyribonucleotides, 600 nM each of the primers, and 600 nM IgLλLUP. Primer sequences for IgLκ were 5′-TGA GCA AAG CAG ACT ACG AGA-3′ (forward) and 5′-GGG GTG AGG TGA AAG ATG AG-3′ (reverse); for IgLλ, primer sequences were 5′-GAG CCT GAC GCC TGA G-3′(forward) and 5′-ATT GAG GGT TTA TTG AGT GCA G-3′ (reverse).

Real-time PCR was performed in a LightCycler (Roche Diagnostics) using the thermocycler program: 3 min of preincubation at 95 °C followed by 50 cycles for 0 s at 95 °C, 10 s at 55 °C, and 11 s at 74 °C. Fluorescence was monitored (excitation at 470 nm and emission at 530 nm) at the end of the annealing phase (the LightCycler F1 channel). All amplification curves were baseline-adjusted by subtracting the arithmetic average of the five lowest fluorescence read-out values in each sample (arithmetic baseline adjustment in the LightCycler software). The threshold was set to a value of 1.00, which was significantly above background noise, and the number of cycles required to reach this values, CT, was determined (11).

MODEL FOR THE QUANTIFICATION OF RELATIVE EXPRESSION OF TWO GENES

A mathematical model was developed to determine the ratio of the expression of two genes by real-time PCR. The model is general and applied here to the IgLκ and IgLλ genes. The basic equation describing real-time PCR amplification is:

$$N_{CT} = N_0 \cdot (1 + E)^{CT} \qquad (1)$$

where N_0 is the number of cDNA molecules, E is the PCR efficiency (E = 1 corresponds to 100% efficiency and is expressed in percentage throughout this work), CT is the threshold cycle number, and N_{CT} is the number of template copies present after CT PCR cycles. E is assumed to be independent of N in the particular amplification range. It is determined by performing a dilution series of mRNA or cDNA calibrator and is calculated from the slope of a plot of CT vs log N_0:

$$E = 10^{-(\text{slope})^{-1}} - 1 \qquad (2)$$

The fluorescence increase (*I*), i.e., the fluorescence signal after subtraction of background, at threshold is proportional to the amount of target DNA:

$$I = k \cdot N_{CT} \qquad (3)$$

where *k* is a system and instrument constant, and N_{CT} is the number of target DNA molecules present at threshold. The relative expression of the IgLκ and IgLλ genes is obtained as:

$$N_{CT_{IgL\kappa}} = N_{0_{IgL\kappa}} \cdot (1 + E_{IgL\kappa})^{CT_{IgL\kappa}} \qquad (4)$$

$$I_{IgL\kappa} = k_{IgL\kappa} \cdot N_{CT_{IgL\kappa}} \qquad (5)$$

$$N_{CT_{IgL\lambda}} = N_{0_{IgL\lambda}} \cdot (1 + E_{IgL\lambda})^{CT_{IgL\lambda}} \qquad (6)$$

$$I_{IgL\lambda} = k_{IgL\lambda} \cdot N_{CT_{IgL\lambda}} \qquad (7)$$

At threshold, $I_{IgL\kappa} = I_{IgL\lambda}$. Equating Eq. 5 with Eq. 7 and rearranging we obtain:

$$K_{RS} = \frac{k_{IgL\lambda}}{k_{IgL\kappa}} = \frac{N_{CT_{IgL\kappa}}}{N_{CT_{IgL\lambda}}} \qquad (8)$$

where the relative sensitivity, K_{RS}, reflects the difference in the probes' fluorescence and binding efficiencies in the two assays. Inserting Eqs. 4 and 6 and rearranging we get:

$$\frac{N_{0_{IgL\kappa}}}{N_{0_{IgL\lambda}}} = K_{RS} \cdot \frac{(1 + E_{IgL\lambda})^{CT_{IgL\lambda}}}{(1 + E_{IgL\kappa})^{CT_{IgL\kappa}}} \qquad (9)$$

This is the central equation to calculate the ratio between the numbers of copies of two cDNA molecules. $CT_{IgL\kappa}$ and $CT_{IgL\lambda}$ are the CT values obtained from the PCR amplifications of the IgLκ and IgLλ cDNAs; $E_{IgL\kappa}$ and $E_{IgL\lambda}$ are the efficiencies of the two PCRs, which are obtained as slopes from plots of CT vs log N_0 in dilution series of the samples; and K_{RS} is the relative sensitivity constant of the two PCR assays, determined using test samples with known cDNA concentrations.

The fractions of IgLκ and IgLλ mRNA, expressed as percentages, are:

$$IgL\kappa = 100 \cdot \frac{K_{RS} \cdot \dfrac{(1 + E_{IgL\lambda})^{CT_{IgL\lambda}}}{(1 + E_{IgL\kappa})^{CT_{IgL\kappa}}}}{1 + K_{RS} \cdot \dfrac{(1 + E_{IgL\lambda})^{CT_{IgL\lambda}}}{(1 + E_{IgL\kappa})^{CT_{IgL\kappa}}}} \qquad (10)$$

$$IgL\lambda = 100 \cdot \frac{1}{1 + K_{RS} \cdot \dfrac{(1 + E_{IgL\lambda})^{CT_{IgL\lambda}}}{(1 + E_{IgL\kappa})^{CT_{IgL\kappa}}}} \qquad (11)$$

Results

EXPERIMENTAL UNCERTAINTY

To classify a sample as either lymphoma-negative with 60:40 IgLκ:IgLλ expression ratio or positive with a deviating expression ratio, we must know with what accuracy CT can be determined. We therefore designed experiments to measure the variation in CT attributable to experimental error and biological variability. We first studied the reproducibility of the PCR by splitting a sample into aliquots that were analyzed in parallel runs (intraassay). We then also included variation attributable to sample handling by analyzing the same sample in independent runs (interassay). To minimize variation in template concentration between the two assays being compared, we prepared a master mixture containing template and all common PCR components and split it into two aliquots to which the unique components for the IgLκ and the IgLλ reactions were added. Each experiment was performed eight times with patient sample BR0 (Fig. 1).

In most reports, PCR reproducibility is expressed as the SD in CT. The variance, SD^2, is:

$$SD^2 = \frac{\sum\limits_{i=1}^{n} (CT_i - \langle CT \rangle)^2}{n - 1} \qquad (12)$$

where $\langle CT \rangle$ is the mean of the measured CT, and SD is the square root of the variance. However, because we are interested in determining the amount of cDNAs in the sample, the SD of $(1 + E)^{-CT}$, which is proportional to the number of cDNA molecules (Eq. 1):

$$N_0 = N_{CT} \cdot (1 + E)^{-CT} \qquad (13)$$

is more relevant. The variance in $(1 + E)^{-CT}$ is:

$$SD^2 = \frac{\sum\limits_{i=1}^{n} \{[(1+E)^{-CT}]_i - \langle (1+E)^{-CT} \rangle\}^2}{n-1} \qquad (14)$$

where $\langle (1 + E)^{-CT} \rangle$ is the mean of $(1 + E)^{-CT}$. To obtain the relative uncertainty in the number of cDNA molecules, we normalize the SD with the average value to obtain the CV, which we express as a percentage:

$$CV = 100 \times \frac{SD}{\langle (1 + E)^{-CT} \rangle} \qquad (15)$$

CV is the uncertainty in the determination of the number of cDNA molecules in the sample attributable to experimental factors.

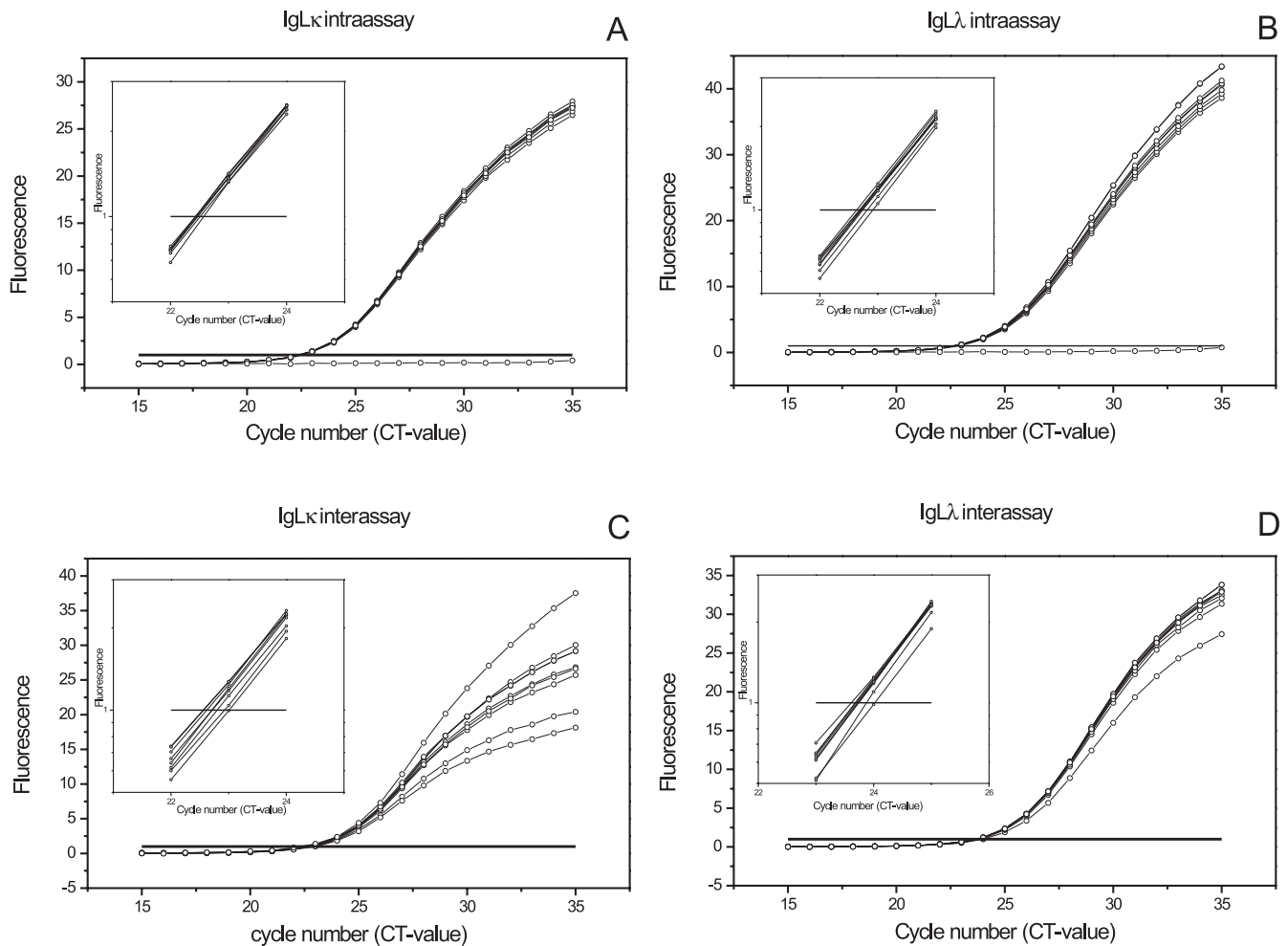The intraassay CV, which reflects the reproducibility of

Fig. 1. Reproducibility of the IgLκ and IgLλ Q-PCR assays.

Shown are the intraassay variations for IgLκ (*A*) and IgLλ (*B*) PCR and the interassay variations for IgLκ (*C*) and IgLλ (*D*) PCR. *Insets* are enlargements in logarithmic scale of the regions where signal intensities crossed the threshold values (CT values).

the PCR, was 3.0% for the IgLκ reaction and 4.9% for the IgLλ reaction (Table 1). The interassay CVs, to which experimental errors also contribute, were only slightly larger: 8.1% for the IgLκ reaction and 5.0% for the IgLλ reaction. Although it was not possible to calculate a CV for the ratio of the two cDNAs, we can estimate how much the IgLκ:IgLλ expression ratio in a negative sample could deviate from 60:40 because of experimental uncertainty in a bad case {CV(a/b) is in general not equal to

$[CV(a)^2 + CV(b)^2]^{1/2}$, as is frequently inferred in PCR user bulletins}. If we suppose that the number of IgLκ cDNA molecules is overestimated, because of experimental error, by 2 SD and that the number of IgLλ cDNA molecules is also underestimated by 2 SD, then the measured ratio would be $(60/40) \times (1 + 0.162)/(1 - 0.100) = 1.94 = 66/34$. If instead the amount of IgLκ cDNA is underestimated and that of IgLλ cDNA is overestimated, then the measured ratio would be $(60/40) \times (1 - 0.162)/(1 + 0.100) = 1.14 = 53/47$.

Table 1. Variations in CT values for the IgLκ and IgLλ reactions in eight repeated measurements of sample BRO run either in parallel (intraassay) or separately (interassay).

	IgLκ			IgLλ		
	$CT_{max}-CT_{min}$[a]	CV (CT),[b] %	CV (copy),[c] %	$CT_{max}-CT_{min}$[a]	CV (CT),[b] %	CV (copy),[c] %
Intraassay	0.15	0.23	3.0	0.28	0.39	4.9
Interassay	0.37	0.62	8.1	0.25	0.37	5.0

[a] Difference between the highest and lowest measured CT values.
[b] CV in CT values.
[c] CV in copy number.

Hence, because of experimental uncertainty and variation in PCR efficiency attributable to the added components, we expect negative samples to display an IgLκ:IgLλ expression ratio of $53{:}47 < N_{0_{IgL\kappa}}{:}N_{0_{IgL\lambda}} < 66{:}34$.

DETERMINATION OF PCR EFFICIENCIES IN PATIENT SAMPLES

Biological samples frequently contain PCR inhibitors, such as heme *(12)*, heparin *(13)*, and IgG *(14)*, and inhibition may vary substantially among samples *(15, 16)*. To correctly interpret results of real-time PCR measurements, it is crucial to estimate the PCR efficiency with high precision in the particular biological sample studied; even a small error in the assumed PCR efficiency may cause large errors in the estimated number of cDNA molecules. We have therefore designed an approach to determine the efficiencies of PCR reactions in situ in biological samples. By diluting the test sample in steps and measuring the CT value at each dilution, we could construct an intrinsic calibration curve from which the PCR efficiency could be determined (Fig. 2). We chose to dilute the samples 64 times, in three fourfold dilution steps. The dilutions were performed in duplicate, and the CT values were measured for both the IgLκ and IgLλ reactions to determine the efficiencies of the two assays separately. Seven patient samples, four negative and three positive, were characterized this way, as well as purified template that should not contain any inhibitors.

The PCR efficiencies obtained when we amplified purified template were $E_{IgL\kappa} = 95\%$ and $E_{IgL\lambda} = 93\%$, signifying that both reactions proceeded with very high efficiencies as expected for optimized PCR assays. Six of the patient samples exhibited efficiencies that were ~10% lower; the IgLλ PCR efficiency was $75\% < E_{IgL\lambda} < 86\%$ with $\langle E_{IgL\lambda} \rangle = 79\%$, and the IgL$\kappa$ efficiency was $79\% < E_{IgL\kappa} < 91\%$ with $\langle E_{IgL\kappa} \rangle = 85\%$ (Table 2). The seventh

Table 2. PCR efficiencies of the IgLκ and IgLλ reactions in test samples and purified template, and relative sensitivity determined in negative samples.

Patient sample	IgLκ		IgLλ		$\dfrac{1+E_{IgL\kappa}}{1+E_{IgL\lambda}}$	$K_{RS}{}^{c}$
	CT[a]	E[b]	CT[a]	E[b]		
BR0	21.0	79.4	21.7	76.8	1.014	1.42
BR18	17.2	86.6	18.8	75.2	1.065	
BR37	22.2	84.2	20.8	75.7	1.048	1.84
BR42	18.7	90.4	17.9	84.4	1.033	1.41
BR46	17.1	82.8	16.4	77.9	1.028	1.42
BR52	21.9	88.7	17.9	85.8	1.015	
Mean		85.4		79.3	1.034	1.52
Template[d]		94.7		93.2	1.008	
BR17	23.1	83.0	23.3	58.9	1.152	

[a] Undiluted samples.
[b] PCR efficiencies calculated from the slopes of plots CT vs log(cDNA concentration) (Fig. 2).
[c] Relative sensitivity (K_{RS}) from Eq. 9 assuming $N_{0_{IgL\kappa}}/N_{0_{IgL\lambda}} = 1.5$.
[d] Purified template.

sample, BR17, exhibited typical IgLκ efficiency (83%), whereas the IgLλ efficiency was only 59%. The reason for the extremely low efficiency of the IgLλ reaction in this sample is unclear. It was considered an outlier and was not included in the calculation of average efficiencies.

When comparing the yields of two reactions, the efficiency ratio:

$$X_{ER} = \frac{(1+E_{IgL\kappa})}{(1+E_{IgL\lambda})} \qquad (16)$$

is the relevant parameter (see Eq. 9). For the six samples, $1.01 < X_{ER} < 1.07$ with $\langle X_{ER} \rangle = 1.03$ (Table 2). Hence, after ~25 amplification cycles, which was typically required to reach threshold with the patient samples (Fig. 1), twice $(1.03^{25} = 2)$ as many κ DNA molecules had been formed
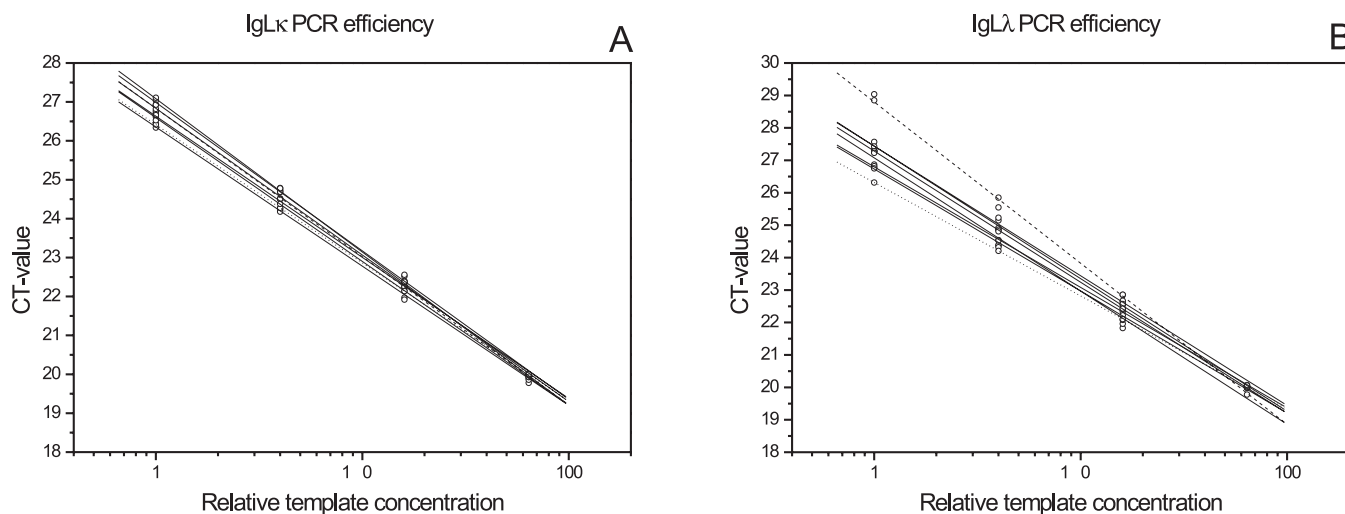

Fig. 2. Efficiencies of IgLκ (*A*) and IgLλ (*B*) PCR assays.

The *lines* are normalized at maximum template concentrations. PCR efficiencies are obtained from the slopes of the *fitted lines* as: $E = 10^{-(slope)^{-1}} - 1$. The outlier, sample BR17, is indicated with a *dotted line*. Purified template is shown with a *dashed line*. For all lines, $R^2 > 0.99$.

compared with λ DNA because of the difference in PCR efficiencies.

Finally, to relate the measured CT values of the two real-time PCRs to the ratio between the numbers of corresponding cDNA molecules, we must also determine the relative sensitivity, K_{RS}, of the two probing systems (Eq. 8).

$$K_{RS} = \frac{N_{0_{IgL\kappa}}}{N_{0_{IgL\lambda}}} \cdot \frac{(1 + E_{IgL\kappa})^{CT_{IgL\kappa}}}{(1 + E_{IgL\lambda})^{CT_{IgL\kappa}}} \quad (17)$$

K_{RS} can be determined by use of IgLκ and IgLλ calibrators. For our purpose, however, it is better to calculate K_{RS} from the CT values ($CT_{IgL\kappa}$ and $CT_{IgL\lambda}$) and PCR efficiencies ($E_{IgL\kappa}$ and $E_{IgL\lambda}$) determined for the four negative samples (Table 2), assuming an IgLκ:IgLλ expression ratio of 60:40. The reason is that the assumption of a particular IgLκ:IgLλ expression ratio will cancel when calculating the relationship between $CT_{IgL\kappa}$ and $CT_{IgL\lambda}$ for negative samples (see below). This gave $1.4 \leq K_{RS} \leq 1.9$ with $\langle K_{RS} \rangle$ = 1.5 (Table 2). Hence, assuming an IgLκ:IgLλ expression ratio of 60:40, the probing of IgLκ DNA is ~50% more sensitive than the probing of IgLλ DNA with the probes and conditions here.

CHARACTERIZATION OF PATIENT SAMPLES

A total of 32 patient samples were analyzed for B-cell lymphoma by the Q-PCR assay. Twelve of the samples were collected as fine-needle aspirates. All samples were run in duplicate, including negative controls. The data are summarized in Table 3 and in Table 1 of the Data Supplement (available with the online version of this article at http://www.clinchem.org/content/vol49/issue1/) and are plotted in Fig. 3. In the plot, each symbol represents one sample and is positioned on the coordinates $CT_{IgL\kappa}$, $CT_{IgL\lambda}$. The corresponding number of cDNA molecules of purified template, calculated assuming $E_{IgL\kappa}$ = 95% and $E_{IgL\lambda}$ = 93%, is indicated in logarithmic scale on the opposite axes. Samples considered negative by IHC analysis are shown as circles, and positive samples are shown as squares.

Negative samples with an IgLκ:IgLλ gene expression ratio of 60:40 are expected to lie on a straight line. Rewriting Eq. 9, we get:

$$N_{0_{IgL\kappa}} \cdot (1 + E_{IgL\kappa})^{CT_{IgL\kappa}} = K_{RS} \cdot N_{0_{IgL\lambda}} \cdot (1 + E_{IgL\lambda})^{CT_{IgL\lambda}} \quad (18)$$

Table 3. Summary of patient sample classification by real-time PCR.

Sample[a]	No. of samples	Correctly classified samples
Lymphadenitis	16	16 (100%)
B-cell lymphoma	15	13 (87%)[b]
T-cell lymphoma	1	0 (0%)

[a] Information about individual patient samples is provided in Table 1 of the Data Supplement.

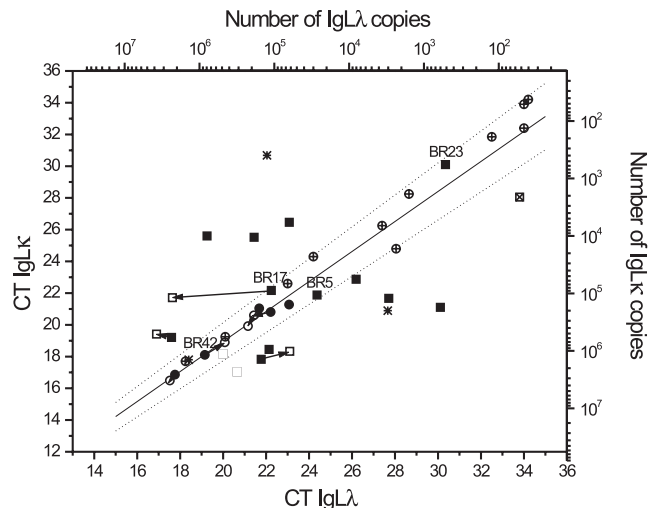[b] BR17 was found lymphoma-positive after in situ calibration.

Fig. 3. Patient samples shown in a plot of $CT_{IgL\kappa}$ vs $CT_{IgL\lambda}$.

Each *symbol* represents one sample and is depicted at its $CT_{IgL\kappa}$ and $CT_{IgL\lambda}$ values. The *top x* and *right y axes* indicate the number of cDNA copies for purified template. The *solid line* represents ($CT_{IgL\kappa}$, $CT_{IgL\lambda}$) values expected for negative samples calculated assuming 85% and 79% PCR efficiencies for the IgLκ and the IgLλ reactions, respectively. The *dotted lines* indicate an interval within which negative samples should be found with at least 95% probability. ■, B-cell lymphomas; ∗, diffuse large B-cell lymphomas; ●, negative samples. □ and ○ indicate corrected CT values for samples for which specific PCR efficiencies were determined. ⊕ and ⊠ indicate fine-needle aspirates. *Arrows* connect measured and corrected CT values for individual samples.

converting it to logarithmic form:

$$CT_{IgL\kappa} \cdot \log(1 + E_{IgL\kappa}) = \log\left(K_{RS} \cdot \frac{N_{0_{IgL\lambda}}}{N_{0_{IgL\kappa}}}\right) + CT_{IgL\lambda} \cdot \log(1 + E_{IgL\lambda}) \quad (19)$$

and rearranging, we obtain:

$$CT_{IgL\kappa} = \frac{\log(1 + E_{IgL\lambda})}{\log(1 + E_{IgL\kappa})} \cdot CT_{IgL\lambda} + \frac{\log\left(K_{RS} \cdot \frac{N_{0_{IgL\lambda}}}{N_{0_{IgL\kappa}}}\right)}{\log(1 + E_{IgL\kappa})}$$

$$= b \cdot CT_{IgL\lambda} + m \quad (20)$$

This describes a linear relationship between $CT_{IgL\kappa}$ and $CT_{IgL\lambda}$ with slope b and intercept m. Inserting $\langle E_{IgL\kappa} \rangle$ = 0.85, $\langle E_{IgL\lambda} \rangle$ = 0.79, and $\langle K_{RS} \rangle$ = 1.5, which are the average values determined for the six samples above (Table 2), and $N_{0_{IgL\kappa}}/N_{0_{IgL\lambda}}$ = 60:40 = 1.5, we obtain b = 0.95 and m = 0.021. Note that the relative sensitivity, K_{RS}, was calculated from measurements on negative samples assuming a 60:40 expression ratio (Eq. 17). This cancels the $N_{0_{IgL\kappa}}/N_{0_{IgL\lambda}}$ ratio in the second term. Hence, the calculated slope and intercept of the relationship between $CT_{IgL\kappa}$ and $CT_{IgL\lambda}$ for negative samples is independent of the assumption of a particular IgLκ:IgLλ expression ratio. A line with b = 0.95 and m = 0.021 is shown in Fig. 3.

Some negative samples were slightly off the line representing 60:40 expression (Fig. 3). This may be attributable to variations in PCR efficiencies among the samples. Such variations can cause an error in the estimation of the

number of cDNA molecules from the measured CT values when mean PCR efficiencies are assumed. If the efficiencies of the two PCR assays in a sample deviate from the mean values to about the same degree, the measured CT values will still correctly reflect the expression ratio and negative samples will fall on the 60:40 line, although they will be displaced diagonally from where they would be if their efficiencies were $\langle E_{IgL\kappa} \rangle$ and $\langle E_{IgL\lambda} \rangle$. However, if the efficiency of one of the reactions deviates more than the other from the mean values, a negative sample may be off the 60:40 line. For the seven samples characterized by in situ calibration (Table 2), the measured CT values could be corrected for the differences between their specific PCR efficiencies and the mean efficiencies:

$$CT_{corr} = CT_{meas} \cdot \frac{\log(1 + E)}{\log(1 + \langle E \rangle)} \qquad (21)$$

The corrected CT values are shown in Fig. 3 with open symbols, and they are connected to the measured CT values by arrows. Indeed, most arrows, sample BR17 being the only exception, are diagonal, indicating that the two reactions are inhibited to the same degree, which does not affect classification.

To account for experimental error and variations in PCR efficiencies in classification of samples, we estimated limits within which negative samples should be found. Keeping the intercept fixed in Eq. 20:

$$CT_{IgL\kappa} = \frac{\log(1 + E_{IgL\lambda})}{\log(1 + E_{IgL\kappa})} \cdot CT_{IgL\lambda} + \frac{\log\left(K_{RS} \cdot \dfrac{N_{0_{IgL\lambda}}}{N_{0_{IgL\kappa}}}\right)}{\left\langle \log(1 + E_{IgL\kappa}) \right\rangle} \qquad (22)$$

we calculated the SD of the slope, $b = \log(1 + E_{IgL\lambda})/\log(1 + E_{IgL\kappa})$, from the efficiencies determined for the six samples (BR17 was excluded) characterized by in situ calibration. This gave an SD of 0.031. For a gaussian distribution, the 95% confidence region is given by the mean $\pm 1.96 \cdot$ SD. In Fig. 3, the dashed lines enclose the region defined by:

$$CT_{IgL\kappa} = (0.95 \pm 0.06) \cdot CT_{IgL\lambda} + 0.021 \qquad (23)$$

Although the confidence region takes into account most of the experimental variation, it accounts for neither the variance in the intercept nor the natural variation in the IgLκ:IgLλ expression ratio among healthy individuals. These factors would broaden the confidence region further. Hence, the region indicates where negative samples are expected to be found with at least 95% probability. All negative samples in this study fell within this region (Fig. 3).

Positive samples with IgLκ clonality were below the 60:40 line, whereas those with IgLλ clonality were above it. This separation of clonal and normal samples was as good for fine-needle aspirates as for the surgical biopsies, although the former contained less material and had

higher CT values. Most positive samples fell outside the confidence region. However, samples BR5 and BR17 were within the region although they were positive. BR17 had anomalous IgLλ PCR efficiency, and when corrected for that, it fell outside the region. We do not know why sample BR5 was within the region. It may have also been attributable to anomalous PCR efficiencies, or it could have been the result of limited clonality. Three samples, indicated by $*$ in Fig. 3, were classified as diffuse large B-cell lymphomas by IHC analysis. One of them, BR29, was close to the 60:40 line. The other two were correctly assayed as positive; one with IgLκ clonality and the other with IgLλ clonality. BR23 was a T-cell lymphoma, as judged by IHC analysis, and the sample therefore exhibited a normal IgLκ:IgLλ ratio. An interactive Excel sheet to analyze IgLκ and IgLλ expression data has been made available as part of the Data Supplement accompanying the online version of this article (http://www.clinchem.org/content/vol49/issue1/) and at http://www.molbiotech.chalmers.se/research/mk/anders/index.htm.

Discussion

We have developed an approach to determine the relative expression of two genes by real-time PCR. We used it to assay for B-cell lymphomas in human samples by measuring the relative expression of IgLκ and IgLλ mRNA. The ratio between IgLκ- and IgLλ-producing cells in healthy individuals was ~60:40, and we expect a similar IgLκ:IgLλ ratio for negative samples in our real-time PCR assay. In lymphoma-derived samples, the IgLκ:IgLλ ratio is expected to deviate substantially from 60:40 because of clonal expansion. In contrast to most other assays based on relative gene expression measurements, this one does not rely on comparison with the expression of housekeeping genes, which has been seriously questioned (17–19).

PCR IN BIOLOGICAL SAMPLES IS SUBSTANTIALLY INHIBITED AND THE DEGREE OF INHIBITION VARIES AMONG SAMPLES AND DEPENDS ON TEMPLATE

In most studies of gene expression by Q-PCR, the CT values determined for test samples have been related to CT values of standard samples containing known amounts of cDNA. This approach relies on the crucial assumption that PCR efficiencies in the test and standard samples are the same. If this is not true, a CT value measured in a test sample will correspond to a different number of cDNA copies than the same CT value measured in the standard sample. The error introduced by such an assumption may be substantial because of accumulation effects. For example, 80% efficiency in the test sample and 85% efficiency in the standard sample produces a 50% difference in the number of DNA copies after 25 cycles (Eq. 1). The common procedure to account for differences in PCR efficiencies between test and standard samples is to amplify a reference gene, usually a housekeeping gene, in parallel and to relate the expression of

the gene being studied to the expression of the house-keeping gene. This, of course, relies on the assumption that expression of the housekeeping gene is constant among the samples being compared, which has also been questioned *(17–19)*. Furthermore, which is rarely acknowledged, it also assumes that the efficiencies of the two reactions, i.e., the PCR of the studied gene and the PCR of the housekeeping gene, are inhibited to the same degree in the standard sample as well as in the test sample *(20)*:

$$\frac{(1 +E\ ^{\text{test sample}}_{\text{test gene}})}{(1 +E\ ^{\text{test sample}}_{\text{housekeeping gene}})} = \frac{(1 +E\ ^{\text{standard sample}}_{\text{test gene}})}{(1 +E\ ^{\text{standard sample}}_{\text{housekeeping gene}})} \quad (24)$$

This critical assumption has, to our knowledge, not been scrutinized. Although one might be inclined to think that inhibitory components that may be present in biological samples should have the same effect on all PCRs, it is not necessarily so. The degree of inhibition may depend on features that are particular for the different PCR systems, such as the length and sequence of template, template tertiary structure, and lengths and sequences of primers. Inhibition may also be indirect through competition for critical elements such as ions and deoxynucleotide triphosphates (dNTPs). The two PCR systems designed here obtain optimum efficiencies at different concentrations of Mg^{2+}, dNTPs, primers, and probe (5 mM $MgCl_2$, 0.2 mM dNTPs, 800 nM primers, and 800 nM probe vs 3.5 mM $MgCl_2$, 0.4 mM dNTPs, 600 nM primers, and 600 nM probe), and elements in biological samples that interact with these PCR components are expected to interfere with the reactions to different degrees.

The PCR efficiencies of both reactions in seven samples and of purified template were determined in situ from CT values measured in dilution series. The total dilution was 64 times, which was sufficient to make the effect of experimental variation in CT values on the slopes of the CT-vs-log(cDNA concentration) plots negligible. Significant PCR inhibition in the biological samples was evident from the significantly higher PCR efficiencies obtained with purified template compared with those obtained in patient samples: purified template had efficiencies >93% compared with efficiencies in the range 75–95% for 13 of the 14 reactions in the patient samples. The IgLλ reaction in sample BR17 was extensively inhibited, with an efficiency of only 59%. The IgLκ reaction in the same sample had the expected efficiency (83%; see Table 2), suggesting that the sample contained components that predominantly interfered with the IgLλ PCR. We did not investigate the cause of inhibition but considered the sample an outlier and did not include it when calculating average efficiencies.

CLASSIFICATION OF SAMPLES
The most accurate classification of samples as lymphoma-negative or -positive is expected when sample-specific inhibition of both PCR reactions is determined by in situ

calibration and accounted for. For the seven samples characterized this way, the fractions of IgLκ expression calculated directly from the measured CT values, i.e., without correcting for sample-specific effects, were 52% (BR0), 59% (BR46), 60% (BR42), and 63% (BR37) in the negative samples and 24% (BR18), 43% (BR17), and 89% (BR52) in the positive samples (Table 1 in the Data Supplement). Because lymphoma-negative samples should express IgLκ to ~60% *(1, 2)*, BR46, BR42, and BR37 are clearly negative, whereas BR18 and BR52 are positive. Classification of BR0 and BR17 is less clear, although the negative BR0 sample expressed IgLκ to a higher extent than the positive BR17 sample (52% vs 43%). When sample-specific efficiencies, as determined by in situ calibration, were taken into account, IgLκ expression in the negative samples was 56%, 62%, 62%, and 62%, whereas it was 6%, 16%, and 93% in the positive samples. The negative samples are thus clearly distinguished from the positive ones, as also seen in Fig. 3, where they are clearly separated by the confidence region based on at least 95% probability.

We did not optimize the in situ calibration protocol in this work, but decided rather arbitrarily to dilute 64 times in steps of 4 and to choose samples containing sufficient material to avoid any statistical uncertainty *(21, 22)*. Note that the in situ calibration protocol is economic with sample because it is based on dilution; less material is required, for example, than when running regular duplicate or triplicate samples. We performed the dilution in four steps, which means that four measurements were made on each sample. Although the samples were run in parallel, some additional hands-on time was required. For high-throughput analyses, it may therefore be time-efficient to first perform a standard single or duplicate measurement on each sample, do a gross classification, and then further characterize uncertain samples by in situ calibration. The gross classification can be quite accurate if any differences in average efficiencies and sensitivities of the two assays are considered. Fig. 3 shows such classification of the samples studied here. All negative samples are within the confidence region, whereas most positive ones are outside it. Three samples in Fig. 3 are false negatives. Two of them are at the periphery of the confidence region and therefore candidates for reinvestigation by the more accurate in situ calibration protocol. Indeed, BR17 was reinvestigated and found to be positive. The positive sample that appears as false negative and is not at the periphery is a diffuse large B-cell lymphoma. The reason for its misclassification has not been identified. It may be attributable to tumor sampling error or highly anomalous PCR efficiencies. However, some diffuse large B-cell lymphomas express very low amounts of immunoglobulins, and the monoclonal immunoglobulin production of the tumor cells may not be detected against the background of polyclonal immunoglobulin produced by nonlymphoma B-lymphocytes in the sample. The classification presented takes into account experimental uncer-

tainty, but to evaluate the individual variation that may be present in various types of NHL a larger series of tumors must be characterized.

The described real-time PCR assay compares the expression of IgLκ and IgLλ and is designed to detect B-cell monoclonality in NHL. This is not sufficient for general tumor screening of patient samples, but demonstrates the potential, accuracy, and effectiveness of real-time PCR-based assays. When more markers are available, real-time PCR-based methods may have great potential as an important complement to morphologic and immunologic methods in clinical tumor diagnostics. Accurate analysis of fine-needle aspirates with a yield of 1000–100 000 representative cells is clearly sufficient for successful analysis. Indeed, we estimate that the material in a fine-needle aspirate will be sufficient for up to 50 different tests to detect various tumor cell characteristics, including B-cell monoclonality.

References

1. Levy R, Warnke R, Dorfman RF, Haimovich J. The monoclonality of human B-cell lymphomas. J Exp Med 1977;154:1014–28.
2. Barandun S, Morell A, Skvaril F, Oberdorfer A. Deficiency of κ- or λ-type immunoglobulins. Blood 1976;47:79–89.
3. Walker NJ. A technique whose time has come [Review]. Science 2002;296:557–9.
4. Svanvik N, Ståhlberg A, Sehlstedt U, Sjöback R, Kubista M. Detection of PCR products in real time using light-up probes. Anal Biochem 2000;287:179–82.
5. Isacsson J, Cao H, Ohlsson L, Nordgren S, Svanvik N, Westman G, et al. Rapid and specific detection of PCR products using light-up probes. Mol Cell Probes 2000;14:321–8.
6. Harris NH, Jaffe ES, Stein H, Banks PM, Chan JK, Cleary ML, et al. A revised European-American classification of lymphoid neoplasms: a proposal from the international lymphoma study group. Blood 1994;84:1361–92.
7. Svanvik N, Nygren J, Westman G, Kubista M. Free-probe fluorescence of light-up probes. J Am Chem Soc 2001;123:803–9.
8. Svanvik N, Westman G, Wang D, Kubista M. Light-up probes. Thiazole orange-conjugated peptide nucleic acid for detection of target nucleic acid in homogeneous solution. Anal Biochem 2000; 281:26–35.
9. Gallagher SR. Quantitation of DNA and RNA with absorption and fluorescence spectroscopy. In: Ausubel FM, Brent R, Kingstone R, Moore DD, Seidman JG, Smith JA, Struhl K, eds. Current protocols in molecular biology. New York: John Wiley & Sons, Inc., 2000: A.3D.2pp.
10. Kubista M, Ståhlberg A, Bar T. Light-up probe based real-time Q-PCR. In: Raghavachari R, Tan W, eds. Genomics and proteomics technologies. Proceedings of SPIE, Vol. 4264. Bellingham, WA: International Society of Optical Engineering, 2001:53–8.
11. Higuchi R, Fockler C, Dollinger G, Watson R. Kinetic PCR analysis: real-time monitoring of DNA amplification reactions. Biotechnology 1993;11:1026–30.
12. Akane A, Matsubara H, Nakamura S, Takahashi S, Kimura K. Identification of the heme compound copurified with deoxyribonucleic acid (DNA) from bloodstrains, a major inhibitor of polymerase chain reaction (PCR) amplification. J Forensic Sci 1994;39:362–72.
13. Izraeli S, Pfleiderer C, Lion T. Detection of gene expression by PCR amplification of RNA derived from frozen heparinized whole blood. Nucleic Acids Res 1991;19:6051.
14. Al-Soud WA, Jonsson LJ, Radström P. Identification and characterization of immunoglobulin G in blood as a major inhibitor of diagnostic PCR. J Clin Microbiol 2000;38:345–50.
15. Rossen L, Norskov P, Holmstrom K, Rasmussen OF. Inhibition of PCR by components of food samples, microbial diagnostic assays and DNA-extraction solutions. Int J Food Microbiol 1992;17:37–45.
16. Wilson IG. Inhibition and facilitation of nucleic acid amplification [Review]. Appl Environ Microbiol 1997;63:3741–51.
17. Bustin SA. Absolute quantification of mRNA using real-time reverse transcription polymerase chain reaction assays [Review]. J Mol Endocrinol 2000;25:169–93.
18. Suzuki T, Higgins PJ, Crawford DR. Control selection for RNA quantitation [Review]. Biotechniques 2000;29:332–7.
19. Schmittgen TD, Zakrajsek BA. Effect of experimental treatment on housekeeping gene expression: validation by real-time, quantitative RT-PCR. J Biochem Biophys Methods 2000;46:69–81.
20. Pfaffl MW. A new mathematical model for relative quantification in real-time RT-PCR. Nucleic Acids Res 2001;29:2002–7.
21. Vogelstein B, Kinzler KW. Digital PCR. Proc Natl Acad Sci U S A 1999;96:9236–41.
22. Peccoud J, Jacob C. Theoretical uncertainty of measurements using quantitative polymerase chain reaction. Biophys J 1996;71:101–8.